



Contents lists available at ScienceDirect

# Bioorganic & Medicinal Chemistry Letters

journal homepage: [www.elsevier.com/locate/bmcl](http://www.elsevier.com/locate/bmcl)

## Structure-based optimization of pyrazolo-pyrimidine and -pyridine inhibitors of PI3-kinase

Steven T. Staben<sup>a,\*</sup>, Timothy P. Heffron<sup>a</sup>, Daniel P. Sutherlin<sup>a</sup>, Seema R. Bhat<sup>a</sup>, Georgette M. Castanedo<sup>a</sup>, Irina S. Chuckowree<sup>d</sup>, Jenna Dotson<sup>a</sup>, Adrian J. Folkes<sup>d</sup>, Lori S. Friedman<sup>b</sup>, Leslie Lee<sup>b</sup>, John Lesnick<sup>c</sup>, Cristina Lewis<sup>c</sup>, Jeremy M. Murray<sup>f</sup>, Jim Nonomiya<sup>c</sup>, Alan G. Olivero<sup>a</sup>, Emile Plise<sup>e</sup>, Jodie Pang<sup>d</sup>, Wei Wei Prior<sup>b</sup>, Laurent Salphati<sup>d</sup>, Lionel Rouge<sup>f</sup>, Deepak Sampath<sup>b</sup>, Vickie Tsui<sup>a</sup>, Nan Chi Wan<sup>d</sup>, Shumei Wang<sup>a</sup>, Christian Weismann<sup>f</sup>, Ping Wu<sup>f</sup>, Bing-Yan Zhu<sup>a</sup>

<sup>a</sup> Discovery Chemistry, Genentech, Inc., 1 DNA Way, South San Francisco, CA 94080, USA

<sup>b</sup> Small Molecule Translational Oncology, Genentech, Inc., 1 DNA Way, South San Francisco, CA 94080, USA

<sup>c</sup> Biochemical Pharmacology, Genentech, Inc., 1 DNA Way, South San Francisco, CA 94080, USA

<sup>d</sup> Medicinal Chemistry Department, Piramed Pharma, 957 Buckingham Avenue, Slough, Berkshire SL1 4NL, UK

<sup>e</sup> Drug Metabolism and Pharmacokinetics, Genentech, Inc., 1 DNA Way, South San Francisco, CA 94080, USA

<sup>f</sup> Structural Biology, Genentech, Inc., 1 DNA Way, South San Francisco, CA 94080, USA

### ARTICLE INFO

#### Article history:

Received 27 April 2010

Revised 12 August 2010

Accepted 12 August 2010

Available online 19 August 2010

#### Keywords:

PI3-kinase

Oncology

Structure-based drug design

### ABSTRACT

Starting from HTS hit **1a**, X-ray co-crystallization and molecular modeling were used to design potent and selective inhibitors of PI3-kinase. Bioavailability in this series was improved through careful modulation of physicochemical properties. Compound **12** displayed in vivo knockdown of PI3K pharmacodynamic markers such as pAKT, pPRAS40, and pS6RP in a PC3 prostate cancer xenograft model.

© 2010 Elsevier Ltd. All rights reserved.

Mutation and over-expression of PI3-kinase  $\alpha$ , as well as deletion of its negative regulator PTEN, in a variety of cancers underline the importance of PI3K $\alpha$  in signal transduction of cell growth and proliferation.<sup>1</sup> The inhibition of PI3K as a means to modulate certain cancer types has indeed been an active area of research and the subject of several recent review articles.<sup>2</sup>

Screening of our internal library of small molecules identified **1a** as a sub-micromolar PI3K $\alpha$  inhibitor (Fig. 1A). The prevalence of PI3-kinase inhibitors with a morpholine hinge-binding substructure<sup>3</sup> led us to first modify the 6-substituent to extend (**1b** and **1d**) or hinder (**1c**) the hydrogen-bond acceptor's expected interaction to the hinge residue (Val882 in PI3K $\gamma$ ). To our surprise, these modifications had little effect on the biochemical potency of these particular inhibitors. Even with removal of the acceptor, as in piperidine **1f**, sub-micromolar inhibition was maintained. From this initial SAR, we concluded the morpholine of **1a** was likely not acting as a hinge-binding motif.

Co-crystallization of the most potent molecule from this series (**1d**) with PI3K $\gamma$  confirmed an alternate mode of binding: interac-

tion between hinge-residue Val882 and the pyrazole nitrogen of the pyrazolo-pyrimidine core (Fig. 1B). The increased potency of **1d** relative to the others in this series likely results from an interaction between one of the sulfone oxygens with Lys833.<sup>5</sup> Analysis of the structure encouraged design of 6-substituents to interact with Tyr867 and Asp841, a strategy successful in the development of GDC-0941.<sup>3a</sup>

Table 1 summarizes modifications of the 2-pyrimidyl substituent with the goal of gaining additional polar interactions to increase potency. Hydrogen-bond accepting substituents on the meta-position of 6-phenyl pyrazolopyrimidines brought modest improvements in potency (**2a–2c**). However, this effect was sensitive to steric size or orientation of the hydrogen-bond acceptor (**2d** and **2e**). Larger improvements in biochemical potency were achieved with heterocyclic substitution (**3** and **4**). To our delight, 4-indazolyl substitution at the 6-position of the pyrazolo-pyrimidine core, as in compound **5a**, resulted in single-digit nanomolar inhibition of PI3K $\alpha$ . The proximity of the H-bond accepting indazole nitrogen to back pocket Tyr867 in an X-ray co-crystal structure of **6** explained the increased biochemical potency (Fig. 2). In contrast to the co-crystal structure of GDC-0941, the indazole N–H of **6** does not appear to be in H-bond proximity to Asp841.

\* Corresponding author. Tel.: +1 6504673103.

E-mail address: [stevents@genentech.com](mailto:stevents@genentech.com) (S.T. Staben).

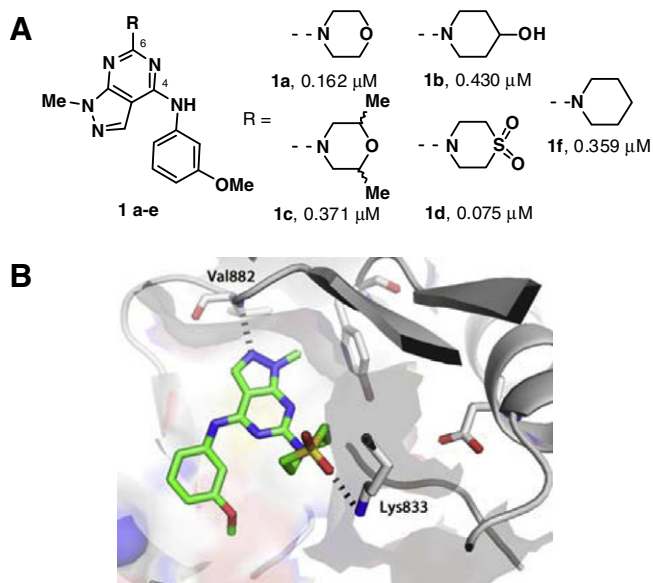


**Figure 1.** (A) PI3K $\alpha$  IC<sub>50</sub> values with changing 2-pyrimidyl substitution. (B) Co-crystal structure of **1d** in PI3K $\gamma$  (PDB id: 3NZS). Potential H-bonding interactions between Val882 and Lys833 are indicated by dashed lines.<sup>4</sup>

**Table 1**  
SAR for 6-pyrazolo-pyrimidine substitution

Entry	Compound	R	PI3K $\alpha$ IC <sub>50</sub> ( $\mu$ M)
1	<b>2a</b>		0.134
2	<b>2b</b>		0.056
3	<b>2c</b>		0.072
4	<b>2d</b>		3.64
5	<b>2e</b>		0.386
6	<b>3</b>		0.029
7	<b>4</b>		0.016
8	<b>5a</b>		0.0014
9	<b>5b<sup>a</sup></b>		0.011
10	<b>5e<sup>a</sup></b>		0.0017

<sup>a</sup> 2,3-Dimethoxyaniline in place of 3-methoxyaniline.

In support of this finding, a 3-aminobenzisoxazole was also a well-tolerated replacement for the indazole, suggesting the indazole N–H is superfluous (compare **5a–5c**).

Potency was maintained when 4-anilino substitution was replaced with more polar alkylamines directed toward the solvent exposed region of the binding site (Table 2). However, pyrazolo-pyrimidines bearing 4-alkylamino substitution typically had clearance higher than hepatic blood flow in rodents (**6–8**). In contrast, 4-anilino substitution typically resulted in molecules with moderate-to-low clearance as exemplified by **9**.

Although **9** displayed moderate clearance in rat (20 mL/min/kg), it was not bioavailable at a 5 mg/kg solution dose (Table 3).<sup>6</sup> Albeit only modestly soluble (7.1  $\mu$ g/mL at pH 6.5), we anticipated the lack of bioavailability of a solution dose was a result of poor

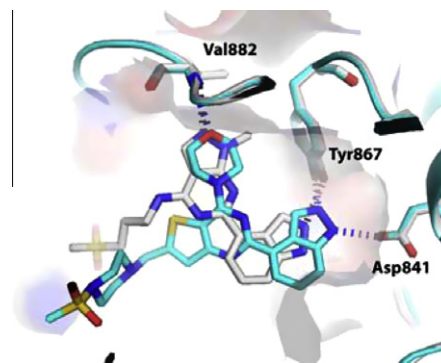


**Figure 2.** Co-crystal structure overlay of **6** (gray, PDB id: 3NZU) and GDC-0941 (cyan, PDB id: 3DBS) in PI3K $\gamma$ . Potential H-bonding interactions between hinge residue Val882 and back pocket residue Tyr867 are indicated by dashed lines.

**Table 2**  
4-Pyrazolo-pyrimidine substitution

Entry	Compound	R	p110 $\alpha$ IC <sub>50</sub> ( $\mu$ M)	Prolif EC <sub>50</sub> <sup>a</sup> ( $\mu$ M)	Rat Cl <sub>p</sub> (mL/min/kg)
1	<b>6</b>		0.0014	0.403	139
2	<b>7</b>		0.0011	ND	103
3	<b>8</b>		0.0083	1.50	176
4	<b>9</b>		0.0014	0.087	20

<sup>a</sup> Proliferation EC<sub>50</sub> determined in an MCF7 cell line. ND = not determined.

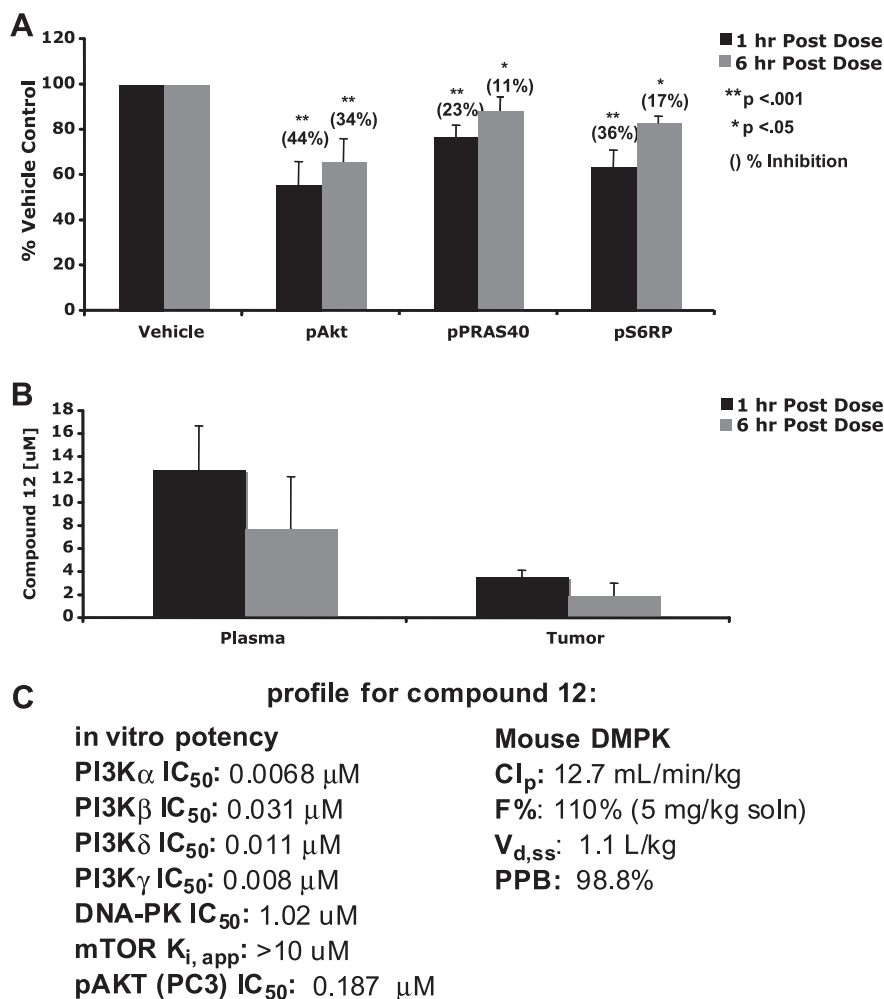
permeability. This anticipation was supported by relatively high TPSA<sup>7</sup> (118 Å<sup>2</sup>) in combination with two hydrogen-bond donors. Indeed **9** exhibited a low apparent permeability in a MDCK permeability assay ( $P_{app\ A-B} = 0.37 \times 10^{-6}$  cm/s, Table 3). Interestingly, the molecule also exhibited pronounced efflux ( $B \rightarrow A/A \rightarrow B = 6.7$ ) which might have affected the bioavailability at low doses.<sup>8,9</sup> This effect was accentuated when tested in both MDR and BCRP transfected MDCK cell lines.<sup>10</sup> We hypothesized that decreasing the TPSA and H-bond donor count might both increase the passive permeability of these molecules as well as alleviate efflux.<sup>11</sup>

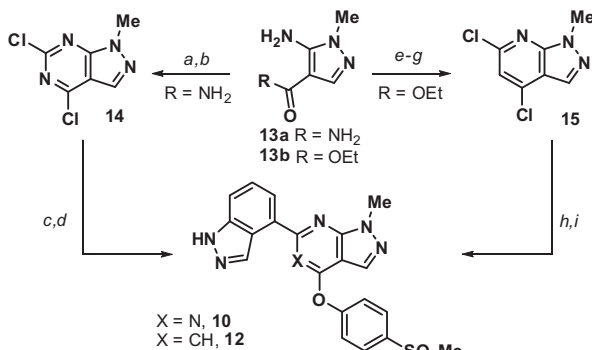
Replacement of the NH with an oxygen atom in aryl ether **10** improves apparent permeability ~sevenfold and reduces efflux in the wild-type, MDR1-transfected and Bcrp1-transfected MDCKI/II cells. Bioavailability is improved substantially. Removal of the linker between the pyrazolo-pyrimidine core and the phenylsulfonyl moiety (**11**) reduces the H-bond donor count and TPSA and provides the most dramatic increase in passive permeability, although at the cost of solubility. It is likely that this extreme increase in permeability also results from a decrease in the number of rotatable bonds in **11**. We sought to further decrease the TPSA of **10** by

**Table 3**

Relationship between physicochemical properties and permeability, solubility, and bioavailability

Compound	X	Y	PI3K $\alpha$ IC <sub>50</sub> ( $\mu$ M)	Donor count	TPSA	$P_{app}$ A–B <sup>a</sup> $\times 10^{-6}$ cm/s (cell line) <sup>b</sup>	B–A/A–B <sup>c</sup>	Solubility pH 6.5 ( $\mu$ g/mL)	Rat Cl <sub>p</sub> (mL/min/kg)	F%
<b>9</b>	NH	N	0.0014	2	118	0.37 (A) 0.13 (B) 0.03 (C)	6.7 79 311	7.1	20	0
<b>10</b>	O	N	0.003	1	115	2.5 (A) 0.8 (B) 0.05 (C)	0.7 4.2–8.8 55.1	16	2.0	29
<b>11</b>	Bond	N	0.0049	1	106	31.5 (A) 7.6 (B) 3.8 (C)	0.5 3.2 4.8	<1	ND	ND
<b>12</b>	O	CH	0.0068	1	102	13.9 (A) 1.2 (B)	0.8 9.3	15	8.4	107

<sup>a</sup>  $P_{app}$  A–B: apparent permeability in the apical to basolateral direction.<sup>b</sup> Cell lines: (A) MDCKI; (B) MDR1-MDCKI; (C) Bcrp1-MDCKII.<sup>c</sup> B–A/A–B =  $P_{app}$  B–A/ $P_{app}$  A–B. ND = not determined. Permeability assays run at 10  $\mu$ M compound concentration.**Figure 3.** (A) Compound **12** displays significant inhibition of PI3K PD markers pAKT (S473), pPRAS40, and pS6 in the PC3 prostate cancer xenograft mouse model (50 mg/kg po, single dose). (B) Plasma and tumor drug levels of compound **12** from 1 to 6 h post dose. (C) Potency and PK profile for **12**.



**Scheme 1.** Synthesis of **10** and **12**. Reagent and conditions: (a) urea, 180 °C, 84%; (b)  $PCl_5$ ,  $POCl_3$ , 150 °C, 64%; (c) 4-(methylsulfonyl)phenol, NaH, THF; (d) 5 mol %  $(PPh_3)_2PdCl_2$ ,  $Na_2CO_3$  (3 equiv), MeCN/ $H_2O$ , 80 °C microwave; (e) dimethylmalonate, NaOEt, EtOH, 100 °C; then (f) 15% NaOH, 100 °C, 60% over (e and f); (g)  $PhP(O)Cl_2$ , 170 °C, 75%; (h) 5 mol %  $(PPh_3)_2PdCl_2$ ,  $NaHCO_3$  (3 equiv), MeCN/ $H_2O$ , 150 °C microwave, 66%; (i) 4-(methylsulfonyl)phenol,  $K_2CO_3$ , DMF, 155 °C microwave, 40%.

removal of a core-nitrogen atom. Through this modification, we anticipated an increase in passive permeability and solubility (esp. at low pH from increased  $pK_a$  of core nitrogen). Pyrazolopyrimidine **12** has a substantially higher apparent permeability, without reduction in solubility, and thus is >100% bioavailable at a 5 mg/kg solution dose.

Importantly, **12** displayed no significant inhibition in a 59-member kinase panel at 1  $\mu M$ <sup>12</sup> and also was selective for class I PI3-kinases over other PIKK family members (i.e., DNA-PK  $IC_{50}$  = 1.02  $\mu M$ , mTOR  $K_{i,app}$  >10  $\mu M$ ). In addition, **12** was not a potent inhibitor of human CYP isozymes ( $IC_{50}$  >20  $\mu M$ ) and was very stable in hepatocyte incubations (human 94% remaining, mouse ~100% remaining, 3 h).

Compound **12** was dosed at 50 mg/kg po in athymic nude mice implanted with PC3-cell xenografts to evaluate its effect on downstream markers of PI3K. Suppression of pAkt, pPRAS40, and pS6RP was observed through the 6 h post dose time period when plasma drug levels remain elevated (Fig. 3).<sup>13</sup>

Synthesis of **10** and **12** is shown in Scheme 1.<sup>14</sup> By slight modification of a literature procedure,<sup>15</sup> heating **13a** in molten urea, followed by  $POCl_3$ -mediated chlorination provided dichloropyrazolopyrimidine **14**. A two-pot procedure was developed for the synthesis of dichloropyrazolopyrimidine **15**. Both **14** and **15** were converted to the titled compounds by standard  $S_NAr$  and Suzuki coupling procedures.

In conclusion, co-crystallization and molecular modeling were used to design analogs of HTS hit **1a** with improved potency. Careful analysis of physicochemical properties led to the identification of specific linker and core modifications that improved passive permeability and minimized efflux leading to dramatically improved bioavailability. Compound **12** displayed a pronounced pharmacodynamic effect on PI3K markers in an in vivo human prostate cancer xenograft model.

## Acknowledgments

The authors thank Mengling Wong, Chris Hamman, Mike Hayes, and Baiwei Lin for analytical/purification support.

## References and notes

- (a) Shayesteh, L.; Kuo, W. L.; Baldocchi, R.; Godfrey, T.; Collins, C.; Pinkel, D.; Powell, B.; Mills, G. B.; Gray, J. W. *Nat. Genet.* **1999**, *21*, 99; (b) Samuels, Y.;

- Wang, Z.; Bardelli, A.; Silliman, N.; Ptak, J.; Szabo, S.; Yan, H.; Gazdar, A.; Powell, S. M.; Riggins, G. J.; Willson, J. K.; Markowitz, S.; Kinzler, K. W.; Vogelstein, B.; Velculescu, V. E. *Science* **2004**, *30*, 554; (c) Parsons, D. W.; Wang, T. L.; Samuels, Y.; Bardelli, A.; Cummins, J. M.; DeLong, L.; Silliman, N.; Ptak, J.; Szabo, S.; Willson, J. K.; Markowitz, S.; Kinzler, K. W.; Vogelstein, B.; Lengauer, C.; Velculescu, V. E. *Nature* **2005**, *436*, 792.
- (a) Hennessy, B. T.; Smith, D. L.; Ram, P. T.; Lu, Y.; Mills, G. B. *Nat. Rev. Drug Disc.* **2005**, *4*, 98; (b) Wee, S.; Lengauer, C.; Wiederschain, D. *Curr. Opin. Oncol.* **2008**, *20*, 77; (c) Chalhoub, N.; Baker, S. J. *Annu. Rev. Pathol. Mech. Dis.* **2009**, *4*, 127; (d) Marone, R.; Cmiljanovic, V.; Giese, B.; Wymann, M. P. *Biochim. Biophys. Acta* **2008**, *159*; (e) Yap, T. A.; Garrett, M. D.; Walton, M. I.; Raynaud, F.; de Bono, J. S.; Workman, P. *Curr. Opin. Pharmacol.* **2008**, *8*, 393; (f) Crabbe, T.; Welham, M. J.; Ward, S. G. *Trends Biochem. Sci.* **2007**, *32*, 460.
- For select examples see: (a) Folkes, A. J.; Ahmadi, K.; Alderton, W. K.; Aliz, S.; Baker, S. J.; Box, G.; Chuckowree, I. S.; Clarke, P. A.; Depledge, P.; Eccles, S. A.; Friedman, L. S.; Hayes, A.; Hancox, T. C.; Kugendradas, A.; Lensun, L.; Moore, P.; Olivero, A. G.; Pang, J.; Patel, S.; Pergl-Wilson, G.; Raynaud, F. I.; Robson, A.; Saghir, N.; Salphati, L.; Sohal, S.; Ultsch, M. H.; Valenti, M.; Wallweber, H. J. A.; Wan, N. C.; Wiesmann, C.; Workman, P.; Zhyvoloup, A.; Zvebil, M. J.; Shuttleworth, S. J. *J. Med. Chem.* **2008**, *51*, 5522; (b) Vlahos, C. J.; Matter, W. F.; Hui, K. Y.; Brown, R. F. *J. Biol. Chem.* **1994**, *269*, 5241; (c) Hayakawa, M.; Kaizawa, H.; Moritomo, H.; Koizumi, T.; Ohishi, T.; Yamano, M.; Okada, M.; Ohta, M.; Tsukamoto, S.-I.; Raynaud, F. I.; Workman, P.; Waterfield, M. D.; Parker, P. *Bioorg. Med. Chem. Lett.* **2007**, *17*, 2438; (d) Hayakawa, M.; Kaizawa, H.; Moritomo, H.; Koizumi, T.; Ohishi, T.; Okada, M.; Ohta, M.; Tsukamoto, S.-I.; Parker, P.; Workman, P.; Waterfield, M. *Bioorg. Med. Chem.* **2006**, *14*, 6847; (e) Rikki, A.; Ahnari, B.; Batchelor, M.; Brookings, D.; Crepy, K.; Crabbe, T.; Deltent, M.-F.; Driessens, F.; Gill, A.; Harris, S.; Hutchinson, G.; Kulisa, C.; Merriman, M.; Mistry, P.; Parton, T.; Turner, J.; Whitcombe, I.; Wright, S. *Bioorg. Med. Chem. Lett.* **2008**, *18*, 4316; (f) Dehnhardt, C. M.; Venkatesan, A. M.; Delos Santos, E.; Chen, Z.; Santos, O.; Ayral-Kaloustian, S.; Brooijmans, N.; Mallon, R.; Hollander, I.; Feldberg, L.; Lucas, J.; Chudhary, I.; Yu, K.; Gibbons, J.; Abraham, R.; Mansour, T. S. *J. Med. Chem.* **2010**, *53*, 798; (g) Zask, A.; Kaplan, J.; Verheijen, J. C.; Richard, D. J.; Curran, K.; Brooijmans, N.; Bennett, E. M.; Toral-Barza, L.; Hollander, I.; Ayral-Kaloustian, S.; Yu, K. *J. Med. Chem.* **2009**, *52*, 7942; (h) Perry, B.; Alexander, R.; Bennett, G.; Buckley, G.; Ceska, T.; Crabbe, T.; Dale, V.; Gowers, L.; Horsley, H.; James, L.; Jenkins, K.; Crepy, K.; Kulisa, C.; Lightfoot, H.; Lock, C.; Mack, S.; Morgan, T.; Nicolas, A.-L.; Pitt, W.; Sabin, V.; Wright, S. *Bioorg. Med. Chem. Lett.* **2008**, *18*, 4700; (i) Sutherlin, D. P.; Sampath, D.; Berry, M.; Castanedo, G.; Chang, Z.; Chuckowree, I.; Dotson, J.; Folkes, A.; Friedman, L.; Goldsmith, R.; Heffron, T.; Lee, L.; Lesnick, J.; Lewis, C.; Mathieu, S.; Nonomiya, J.; Olivero, A.; Pang, J.; Prior, W. W.; Salphati, L.; Sideris, S.; Tian, Q.; Tsui, V.; Wan, N. C.; Wang, S.; Wiesmann, C.; Wong, S.; Zhu, B.-Y. *J. Med. Chem.* **2010**, *53*, 1086; (j) Heffron, T. P.; Berry, M.; Castanedo, G.; Chang, C.; Chuckowree, I.; Dotson, J.; Folkes, A.; Gunzner, J.; Lesnick, J. D.; Lewis, C.; Mathieu, S.; Nonomiya, J.; Olivero, A.; Pang, J.; Peterson, D.; Salphati, L.; Sampath, D.; Sideris, S.; Sutherlin, D. P.; Tsui, V.; Wan, N. C.; Wang, S. M.; Wong, S.; Zhu, B. Y. *Bioorg. Med. Chem. Lett.* **2010**, *20*, 2408.
- X-ray structures of **6** and **1d** have been deposited in the PDB (id: 3NZS and 3NZU).
- Lys833 is not well defined in the crystal structure density. This interaction could be more important in PI3K $\alpha$ .
- No detectable concentration after oral dosing at 5 mg/kg in 80% PEG/EtOH vehicle.
- TPSA (topological polar surface area) calculation similar to that as described in: Ertl, P.; Rohde, B.; Selzer, P. *J. Med. Chem.* **2000**, *43*, 3714.
- (a) Kwon, H.; Lionberger, R. A.; Yu, L. X. *Mol. Pharm.* **2004**, *1*, 455; (b) Lin, J.; Chiba, M.; Bailie, T. *Pharmacol. Rev.* **1999**, *1*, 135; (c) Collett, A.; Tanianis-Hughes, J.; Hallifax, D.; Warhurst, G. *Pharm. Res.* **2004**, *21*, 819.
- Consistent with this statement, co-administration of Gefitinib (a known PgP and BCRP inhibitor) with compound **9** did result in improved bioavailability of **9**.
- This ratio was decreased when co-administered with known inhibitors of PgP (GF120918, Elacridar) and BCRP (Fumitremorgin C). For example:  $P_{app} A-B = 0.63 \times 10^{-6}$  cm/s,  $B-A/A-B = 17.60$  for **9** in cell line C (Bcrp1-MDCKII) in the presence of Fumitremorgin C.
- For examples, see (a) Roberts, L. R.; Bryans, J.; Conlon, K.; McMurray, G.; Stobie, A.; Whitlock, G. A. *Bioorg. Med. Chem. Lett.* **2008**, *18*, 6437; (b) Raub, T. J. *Mol. Pharm.* **2005**, *3*, 3.
- Study performed at Invitrogen; most significant was 27% inhibition of FLT 3.
- The attenuated pathway knockdown for **12** can be attributed to its modest cellular pAKT activity as well as low exposure of free drug in this experiment (mouse plasma protein binding = 98.8%). Compound **12** was not tested in a mouse xenograft model for tumor growth inhibition. Determination of a MTD was not attempted.
- (a) For experimental data and characterization see: Dotson, J.; Heffron, T.; Olivero, A. O.; Sutherlin, D. P.; Staben, S. T.; Wang, S.; Zhu, B.-Y.; Chuckowree, I. S.; Folkes, A. J.; Wan, N. C. WO/2010/059788; PCT/US2009/065085; (b) Dotson, J.; Heffron, T.; Olivero, A. O.; Sutherlin, D. P.; Wang, S.; Zhu, B.-Y.; Chuckowree, I. S.; Folkes, A. J.; Wan, N. C. WO/2009/097446; PCT/US2009/032459.
- Ferroni, R.; Simoni, D.; Orlandini, P.; Bardi, A.; Franze, G. P.; Guarneri, M. *Arzneimittelforschung* **1990**, *40*, 1328.